Percolation Effects in Supercapacitors with Thin, Transparent Carbon Nanotube Electrodes

Paul J. King,[†] Thomas M. Higgins,[†] Sukanta De,[†] Norbert Nicoloso,[‡] and Jonathan N. Coleman[†,*]

[†]School of Physics and CRANN, Trinity College Dublin, Dublin 2, Ireland and [‡]Materials Science, TU Darmstadt, Petersenstr. 32, 64287 Darmstadt, Germany

ABSTRACT

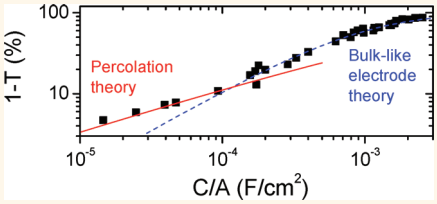

We have explored the effects of percolation on the properties of supercapacitors with thin nanotube networks as electrodes. We find the equivalent series resistance, R_{ESR}, and volumetric capacitance, C_V, to be thickness independent for relatively thick electrodes. However, once the electrode thickness falls below a threshold thickness (~100 nm for R_{ESR} and ~20 nm for C_V), the properties of the electrode become thickness dependent. We show the thickness dependence of *both* R_{ESR} and C_V to be consistent with percolation theory. While this is expected for R_{ESR}, that the capacitance follows a percolation scaling law is not. This occurs because, for sparse networks, the capacitance is proportional to the fraction of nanotubes connected to the main network. This fraction, in turn, follows a percolation scaling law. This allows us to understand and quantify the limitations on the achievable capacitance for transparent supercapacitors. We find that supercapacitors with thickness independent R_{ESR} and C_V occupy a well-defined region of the Ragone plot. However, supercapacitors whose electrodes are limited by percolation occupy a long tail to lower values of energy and power density. For example, replacing electrodes with transparency of $T = 80\%$ with thinner networks displaying $T = 97\%$ will result in a 20-fold reduction of both power and energy density.

KEYWORDS: supercapacitor · nanotube · network · percolation · transparent

The past decade has seen growing interest in flexible electronics, a technology which will be important in areas such as flexible displays, smart labels, animated posters, and portable power generation. Fabricating such technology will involve the deposition, patterning, and integration of all of the elements of electronic circuitry to form electronic devices on flexible plastic substrates. The deposition should be possible at low temperature and be scalable to large areas. Solution-based deposition techniques such as printing or spraying are ideal in this area. One sub-area of this field which has seen a huge effort recently is solution deposition of transparent electrodes for flexible displays or solar cells. To retain conductivity while flexing,[1] networks of nanostructured materials such as nanotubes, graphene, or metallic nanowires have been heavily studied.[2−4] Many believe that the next stage in the development of flexible electronics will require all components of the device to be transparent for use in applications such as transparent displays or heads up displays.[5] For many such applications, transparent energy storage devices will be required.[6] To this end, a number of groups have demonstrated transparent supercapacitors or batteries.[6−11] In general, the research has focused on using nanomaterials to produce thin but high surface area electrodes which can be transparent if made thin enough.[12−14] In the simplest case, these electrodes can then be combined with a suitable electrolyte and separator to produce a supercapacitor.[15]

Electrochemical double-layer capacitors (EDLC), also known as supercapacitors (SC), are devices that store charge and so energy at the interface between a conducting electrode and an electrolyte. To maximize the charge storage capacity (the capacitance), the electrode must have high surface area. It should also be highly conductive to avoid the need for a current collector. Finally, it should be stable in the presence of the electrolyte. Recently, much work has involved porous networks of inert nanoconductors such as nanotubes or graphene.[16−21] This results in a highly conductive, high surface area electrode. In addition, such electrodes can be deposited from solution and tend to be stable under flexing.[1] Transparency can be achieved by making the electrodes extremely thin. To date, a number of papers have described such transparent nanostructured

* Address correspondence to colemaj@tcd.ie.

Received for review December 5, 2011 and accepted January 7, 2012.

Published online January 07, 2012
10.1021/nn204734t

© 2012 American Chemical Society

supercapacitors with specific capacitance from ~25 to >100 F/g.[7,8,10,12]

However, reducing the thickness to increase the transparency brings certain problems. Most obviously, thin films may be resistive and have low absolute capacitances.[22] However, there is a more subtle problem for nanostructured electrodes. For bulk-like materials, intrinsic properties such as DC conductivity and specific capacitance are thickness independent.[23] However, when nanostructured thin films become thin enough, their properties, particularly their electrical properties, become thickness dependent. In practice, this means electrical properties which get progressively worse as the thickness is decreased. This phenomenon is known as percolation and has been heavily studied for decades.[24]

Electrical percolation describes the onset of electrical conductivity across a previously insulating region once conducting links have been added at a density exceeding some critical value, the percolation threshold. For conducting rods, randomly deposited in-plane and above the percolation threshold, the conductivity follows the percolation scaling law, $\sigma_{DC} \propto (N_A - N_{A,C})^{n_{DC}}$, where N_A is the number of rods per unit area, $N_{A,C}$ is the percolation threshold, and n_{DC} is the percolation exponent.[2] This scaling law can also be expressed in term of film thickness, t, rather than conductor density:[25]

$$\sigma_{DC} \propto (t - t_c)^{n_{DC}} \quad (1)$$

Here t_c is the threshold thickness (*i.e.*, the thickness below which no conductive paths exist). As the network thickness is increased above t_c, the network conductivity initially follows eq 1. However, experiments have shown that a second transition thickness, t_{min}, exists, above which the conductivity becomes thickness invariant.[1,26−29]

Percolative behavior has been seen in many papers for networks of nanotubes, nanowires, and graphene nanosheets.[2,26,30] A recent review has cataloged the network transmittance at the percolation to bulk-like transition thickness, t_{min}, for a wide range of published networks.[26] This transmittance varied from ~45 to 92%. This means that, for the majority of networks with technologically relevant transmittance (T > 90%), the electrical conductivity is limited by percolation. While the effects of percolation are well understood for transparent conductors,[26,29,31] they have not been considered in the case of transparent supercapacitors.

In this work, we study the effects of percolation in nanostructured electrodes on supercapacitor performance. We prepare SC electrodes from carbon nanotube networks with a range of thicknesses from ~5 to ~500 nm. By measuring the transmittance and sheet resistance, we demonstrate the presence of both bulk-like and percolative regimes with a transition thickness of ~100 nm. Electrochemical testing shows the equivalent series resistance to be dominated by the electrode resistance and to show percolative behavior for electrode thickness below 100 nm. Most interestingly, we find the volumetric capacitance to be thickness invariant for thick films but demonstrate percolation effects for electrodes with thickness below 20 nm. Finally, we consider what performance can be achieved by highly transparent supercapacitors. We emphasize that the aim of this work is not to demonstrate supercapacitors with superior performance. The aim is to use carbon nanotubes as a model system to demonstrate the effects of percolation on supercapacitors with nanostructured electrodes.

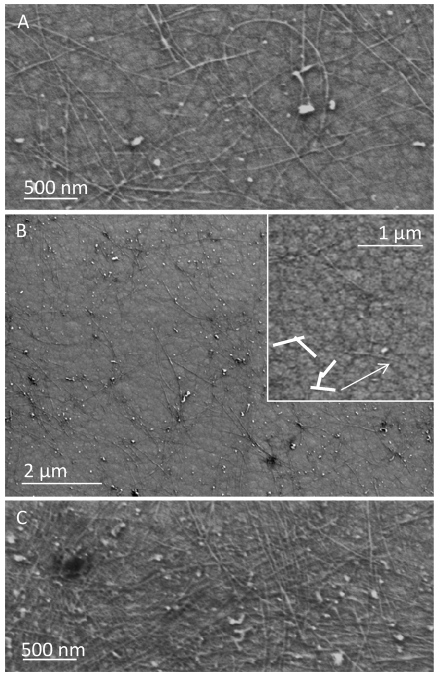

Figure 1. SEM images of nanotube networks. (A) SEM image of a 5 nm thick SWNT film. (B) Wide field image of the same film. Inset: Thin networks such as this contain nanotubes which are isolated or only weakly connected to the network. This is shown in the SEM, although the poor contrast achieved for these sparse networks makes it difficult to see isolated nanotubes. The motif in white is a schematic demonstrating the shape of the array of nanotubes in this image. The arrow links part of the schematic to the equivalent position in the image. (C) SEM image of a 12 nm thick SWNT film.

RESULTS AND DISCUSSION

Bulk to Percolation Transition. The supercapacitor electrodes studied during this work were prepared by vacuum filtration of aqueous carbon nanotube dispersions to give thin nanotube films with a range of thickness from 5 to 500 nm (see below). Shown in Figure 1 are SEM images of very thin films (5 and 12 nm average thickness). To facilitate imaging, these were transferred from the filter membrane to AuPd-coated glass. Figure 1A represents a portion of a 5 nm thick film and shows the nanotubes to be arrayed in bundles (estimated mean diameter and length of 23 nm and

1.3 μm, respectively) which are randomly arranged on the surface. Figure 1B shows a lower magnification image of the same film which demonstrates considerable spatial nonuniformity. While some regions of the film contain clusters of nanotubes, other regions are relatively sparsely populated. Such nonuniformity has been observed before by both Raman mapping and spatially resolved transmittance measurements.[1,25] In addition, the inset illustrates a small cluster of tubes that are only weakly connected (if at all) to the rest of the network. Figure 1C shows a portion of a 12 nm thick film showing a considerably larger nanotube density.

For detailed characterization, the nanotube networks were transferred from the filter membrane to transparent plastic substrates (PET). We performed initial characterization by measuring the optical transmittance spectra and four probe sheet resistances for each film. The transmittance (550 nm) varied from 97 to 13%, while the sheet resistance varied from 10^5 to 10^2 Ω/sq over the same thickness range. The measured transmittance (550 nm) is plotted as a function of sheet resistance in Figure 2A. For thin conducting films, where the DC conductivity is thickness independent, the transmittance is related to the sheet resistance by[2,32]

$$T = \left(1 + \frac{Z_0}{2R_s}\frac{\sigma_{Op}}{\sigma_{DC,B}}\right)^{-2} \quad (2)$$

where $Z_0 = 377\ \Omega$ is the impedance of free space and σ_{Op} and $\sigma_{DC,B}$ are the optical conductivity and the (bulk-like) DC conductivity, respectively. For relatively thick films, $\sigma_{DC,B}/\sigma_{Op}$ is thickness independent and can be used as a figure of merit (FoM), representing a simple way of comparing different samples.[29] This expression can be fitted to the data in Figure 2A, as indicated by the dashed line. A good fit was obtained for films with transmittance $T < 45\%$. This fit gives a value of $\sigma_{DC,B}/\sigma_{Op} \approx 1.9$ for these films, which is typical of the values found for carbon nanotube networks.[26] Given that the optical conductivity of carbon nanotube networks is known to be $\sigma_{Op} = 1.7 \times 10^4$ S/m,[1,33−35] this allows us to estimate the bulk DC conductivity of the thick networks to be $\approx 3 \times 10^4$ S/m.

However, we observe significant deviation from this bulk-like behavior for thin films with $T > 45\%$. As the transmittance is increased above 45%, the thickness falls below t_{min}, and percolative effects begin to control the DC conductivity. Such a transition has been observed for thin films of nanotubes,[1] nanowires,[27] and graphene sheets.[28] We have recently shown that, in the percolation regime, the transmittance is related to the sheet resistance by

$$T = \left[1 + \frac{1}{\Pi}\left(\frac{Z_0}{R_s}\right)^{1/(n_{DC}+1)}\right]^{-2} \quad (3)$$

where Π is known as the percolative FoM and n_{DC} is the percolation exponent (see eq 1). Equation 2 can be fitted to the high T data in Figure 1A. An extremely good fit was obtained for films with $T > 45\%$, yielding $\Pi = 3.1$ and $n_{DC} = 0.6$. Again, these values are typical of nanotube films.[26]

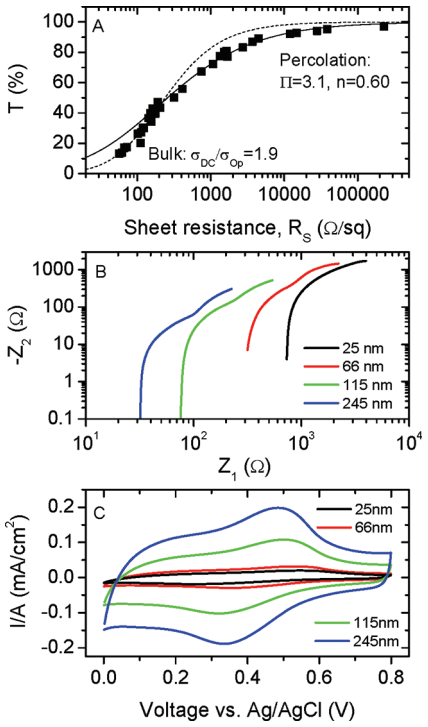

Figure 2. (A) Optical transmittance (550 nm) plotted as a function of sheet resistance for the electrodes (deposited on PET) used in this work. The dashed and solid lines are fits to eqs 2 (bulk) and 3 (percolation), respectively. (B) Nyquist plots and (C) cyclic voltammograms for selected electrode thicknesses.

These data clearly show that percolation effects are present in these thin nanotube films so long as the transmittance is above 45%. Such percolation effects have been observed in many nanostructured networks, with the transition from bulk-like to percolative behavior occurring for networks with transmittances from 45 to 92%.[26] To be incorporated into transparent electronics, components are likely to require $T > 90\%$. Thus, it is clear that technologically relevant network devices will operate in the percolation regime.

Supercapacitor Electrode Thickness Dependence. Thus, it is apparent that, if thin transparent films are to be used as supercapacitor electrodes, percolation will play a limiting role. It will be important to understand how these percolation effects impact upon the capacitance (C) and equivalent series resistance (R_{ESR}) for thin film devices. To test this, we performed electrochemical tests in a three-electrode configuration using our thin nanotube networks (deposited on plastic substrates) as the working electrode. Note that because of this three-electrode configuration our measurements of C and R_{ESR} apply to a single electrode and not to a supercapacitor device. No additional current collectors were used. To quantitatively evaluate the performance

of the electrodes, electrochemical impedance spectroscopy (EIS) and cyclic voltammetry (CV) were performed (electrolyte 1.0 M H_2SO_4). Examples of Nyquist plots for various electrode thicknesses (see below) are shown in Figure 2B. These are typical of nanotube electrodes and consist of a semicircle at high frequency which intercepts with the Z_1 (real) axis to give R_{ESR}. In the low-frequency regime, $-Z_2$ increases almost linearly with Z_1. It is unclear whether this is indicative of the presence of another semicircle or of the presence of a Warburg impedance. Some examples of the CV curves (recorded after 20 cycles) can be seen in Figure 2C (scan rate 50 mV/s). The CV curves are typical of those of carbon nanotubes functionalized with carboxylic acid groups with broad reduction and reoxidation features.[36]

In order to ascertain the effects of percolation, it is necessary to analyze the electrochemical data as a function of film thickness. To do this, the network thickness must be estimated with reasonable accuracy. For thin conducting films, the transmittance scales with thickness as[32]

$$T = [1+Z_0\sigma_{Op}t/2]^{-2} \quad (4)$$

It is well-known that the optical conductivity of carbon nanotube networks is close to $\sigma_{Op} = 1.7 \times 10^4$ S/m.[1,33−35] Using this value and eq 4, we can calculate film thickness from the transmittance data. To illustrate this, we plot the measured film transmittance as a function of calculated thickness in Figure 3A. It is important to note that real capacitors have two electrodes. This means that, if for example, an overall transmittance of $T > 80\%$ is required, then each electrode must have $T > 89\%$. This corresponds to a thickness of $t < 17$ nm and falls well inside the percolation regime. In addition, we plot the sheet resistance data as a function of film thickness in Figure 3B. As expected for bulk-like materials, for the thicker films, R_s scales inversely with thickness as illustrated by the dashed line. However, below a critical thickness, $t_{min,DC} \approx 100$ nm, the data deviate from this line as percolation effects become important. Previously, we showed that the thickness where the bulk to percolation transition occurs is related to the bundle diameter, D, by $t_{min,DC} \approx 2.33D$.[29] That the measured mean bundle diameter is 23 nm predicts that $t_{min,DC} = 54$ nm. The reason for the disagreement is unclear.

We measured the equivalent series resistance from the impedance data for all electrode thicknesses. The thickness dependence of the R_{ESR} is plotted in Figure 3C. It is noteworthy that R_{ESR} displays a thickness dependence almost identical to that of R_s, displaying bulk-like behavior above a thickness of $t_{min,ESR} = 100$ nm but percolative behavior below this transition thickness. We plot R_{ESR} *versus* R_s in the inset of Figure 3C, finding almost perfect linearity. This would

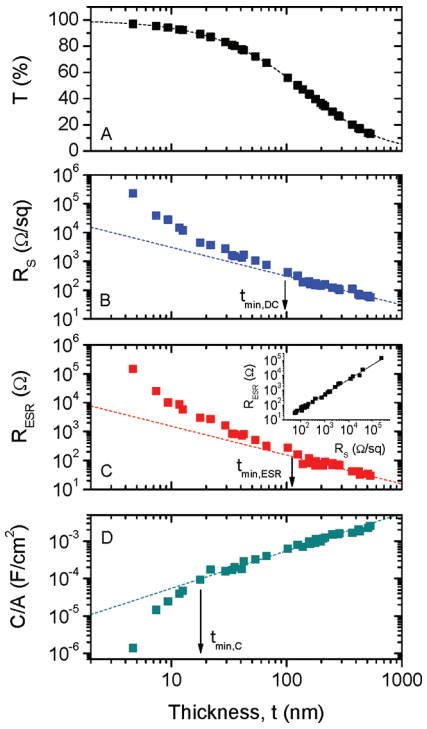

Figure 3. Electrode properties plotted as a function of network thickness, as calculated from the transmittance. (A) Network transmittance, (B) sheet resistance, (C) equivalent series resistance, and (D) capacitance per unit area. Shown in the inset of (C) is a plot of equivalent series resistance *versus* sheet resistance. (B−D) Dashed lines represent the behavior expected for bulk-like electrode. The arrows indicate the point of deviation from bulk-like behavior.

be expected for an electrode where the active material also plays the role of the current collector and the electrolyte resistance is negligible.

The capacitance was determined from the cyclic voltammetry curves. We calculated the electrode capacitance after 20 cycles using $I = CdV/dt$.[22] Note that the current was normalized to the electrode area (constant for all films at 2.83 cm^2) and averaged over the entire potential range to give the capacitance per unit area (C/A) which is plotted against thickness in Figure 3D. For thicknesses above a minimum value ($t_{min,C} \approx 20$ nm), the capacitance scales linearly with thickness as expected for a bulk-like material. It is worth noting that this linear behavior occurs when the electrolyte effectively wets the electrode. This is the case here because the electrolyte is aqueous and the nanotubes making up the electrode are functionalized with carboxylic groups rendering the electrode surface hydrophilic. However, below this threshold, the capacitance falls off more rapidly than expected. This is a significant effect with the thinnest film displaying capacitance an order of magnitude lower than expected. Comparison with the behavior of R_s and R_{ESR} strongly suggests this behavior to be percolative in nature. To the best of our knowledge, this effect has not been reported previously.

While the data described above suggest the presence of percolation effects, such phenomena can be demonstrated more clearly by plotting as a function of thickness a parameter such as DC conductivity, which is normally thickness invariant. To do this, we calculate the DC conductivity of the electrode from the sheet resistance using $\sigma_{DC} = (R_s t)^{-1}$. We can also calculate an effective conductivity associated with the ESR which we define as $\sigma_{ESR} = (R_{ESR} t)^{-1}$. These conductivities are plotted against thickness in Figure 4A. For thicknesses above ~100 nm, we observe both conductivities to be constant within error as would be expected for a bulk-like electrode. However, for thicknesses below ~100 nm, both conductivities tend to fall nonlinearly with decreasing thickness. Similar behavior has been previously observed for thin conducting films of nanostructured materials such as carbon nanotubes,[1,37] graphene,[28] and metallic nanowires.[27,29] We emphasize that the same behavior is observed for the ESR as the DC conductivity because the ESR is dominated by the resistance of the electrode.

We can confirm that this behavior is due to percolation by showing that the conductivity scales with thickness as described by the percolation scaling law (eq 1). This is clearly demonstrated in the inset of Figure 4A for both the DC and effective conductivities at thickness below $t_{min,DC}$ and $t_{min,ESR}$, respectively. From the fits, we find the percolation threshold to be t_c = 4.3 nm in each case. The percolation exponents were n_{ESR} = 0.69 and n_{DC} = 0.66. These values are much smaller than the universal value of 1.3, expected for two-dimensional systems.[24] However, we note that such low values are commonly found for carbon nanotube networks.[26,29] The reason for this discrepancy is unknown.

Similarly, we can explore in more detail the possibility of percolation of capacitance by plotting the capacitance per electrode volume, $C_V = C/At$, as a function of film thickness, as shown in Figure 4B. Assuming that the nanotube network has a well-defined surface area per unit volume, then this volumetric capacitance should be independent of film thickness for a bulk-like film (assuming good electrolyte wetting). As was the case for the conductivity data, we observe constant volumetric capacitance for thicknesses above 20 nm. We denote this constant volumetric capacitance for thick bulk-like films, $C_{V,B}$, which has a mean value of 55 F·cm^{-3}. However, a significant falloff in volumetric capacitance is observed at lower thicknesses. If this falloff is a percolation effect, then we expect the volumetric capacitance to scale with thickness in the thin film regime as

$$C_V \propto (t - t_c)^{n_C} \quad (5)$$

We believe the capacitance will follow this form because a wide range of phenomena described by percolation theory can be modeled using this type of function.[24] However, we will give a more rigorous justification below. The inset of Figure 4B shows this model to fit the data extremely well giving values t_c = 4.3 nm and n_C = 0.83. These values are similar to those obtained for the sheet resistance and ESR. We can use the thick film data to estimate the specific capacitance, taking an estimated network density of 1000 kg/m^3 (as measured for a thick free-standing film). This is displayed on the right axis of Figure 4 and shows the capacitance per unit mass to saturate at ~55 F/g in the bulk-like region. This is in line with a number of papers on nanotube-based transparent supercapacitor electrodes.[7,8,10,12]

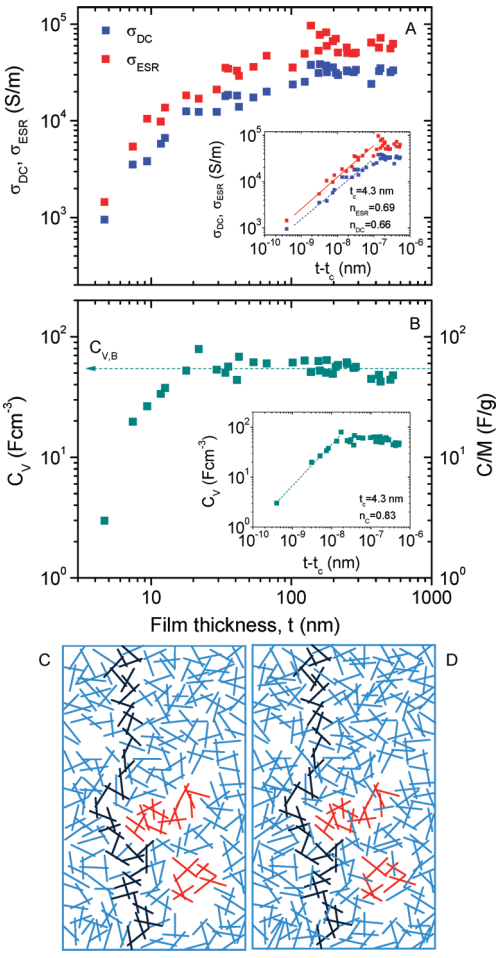

Figure 4. Percolation effects in these electrodes. (A) Electrode DC conductivity (calculated from the sheet resistance) and the equivalent ESR conductivity, defined as $\sigma_{ESR} = (R_{ESR}t)^{-1}$ plotted as a function of film thickness. Inset: the same data plotted as a percolation curve. The fit gives a percolation threshold of t_c = 4.3 nm and percolation exponents of n_{ESR} = 0.69 and n_{DC} = 0.66. (B) Capacitance per film volume plotted as a function of film thickness. The right axis shows the capacitance in F/g (taking ρ = 1000 kg/m^3). Inset: same data plotted as a percolation curve. The fit gives a percolation threshold of t_c = 4.3 nm and a percolation exponents of n_C = 0.83. (C,D) Schematics of random two-dimensional networks of sticks. The stick densities in (C) and (D) are $4.3L^{-2}$ and $4.9L^{-2}$, where L is the mean stick length. In each case, the dark blue sticks illustrate a percolating path, while the red sticks in (C) represent two isolated clusters. In (D), these clusters are now connected to the rest of the network.

It is interesting that while the percolation threshold is the same for DC conductivity, equivalent circuit resistance, and capacitance data (t_c = 4.3 nm) the transition from percolative to bulk-like behavior occurs at a lower thickness ($t_{min,C} \approx 20$ nm) for the capacitance than it does for the sheet resistance or ESR ($t_{min,DC} \approx t_{min,ESR} \approx 100$ nm). It is unsurprising that the percolation threshold should be the same in all cases. The measurements of R_{ESR}, σ_{DC}, and C/A all require current flow in the network, so should all give the same value of t_c.

However, the thickness where percolative behavior transitions to bulk-like behavior, t_{min}, is more subtle. It has been shown previously for nanostructured networks that this transition occurs at the same thickness as a transformation from spatially nonuniform to greater network uniformity.[1,27,28] This transition tends to occur at a network thickness that is ~2.3 times the diameter of the nanowires or nanotubes making up the network.[29] However, the volumetric capacitance is unlikely to be sensitive to the network nonuniformity. More probably, the capacitance is sensitive to the connectivity of the network. For very sparse networks, not all nanotubes will be connected to the main network. We might expect the capacitance to depend on the number of nanotubes that are directly connected to the main network and to become thickness independent when the last isolated nanotube cluster becomes connected to the rest of the network. This is likely to occur significantly before the nonuniformity to uniformity transition in line with what is experimentally observed.

We illustrate this behavior in Figure 4C,D. Figure 4C shows a schematic of a sparse network of randomly arranged sticks. This network is above the percolation threshold as illustrated by the conductive path marked by dark blue sticks. However, it is sparse enough to be quite nonuniform; the bottom right portion has considerably lower stick density than the top right for example. As shown previously, such nonuniformity is associated with thickness dependent DC conductivity and so behavior characteristic of electrical percolation.[1,27,28] In addition, it has a number of clusters (illustrated by red sticks) which are not connected to the rest of the network. These clusters can contribute to neither current flow nor capacitance. Thus we expect this network to have an effective thickness which is below both $t_{min,DC}$ and $t_{min,C}$. Shown in Figure 4D is the same network, but where 50 more sticks have been added randomly. It is clear that this network is still spatially nonuniform. Thus thickness-dependent conductivity is still expected ($t < t_{min,DC}$). However, all sticks are now connected to the network and so can contribute to the capacitance. This suggests that $t > t_{min,C}$. This supports the possibility of a scenario where a network can have thickness such that $t_{min,C} < t < t_{min,DC}$, as suggested by our experiments.

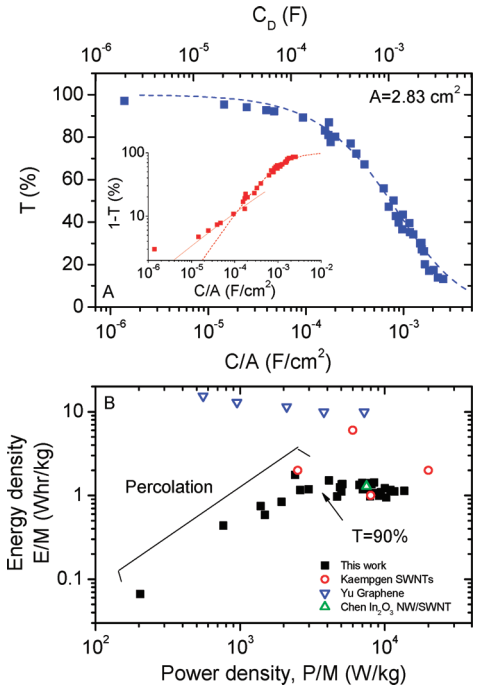

Figure 5. (A) Measured transmittance (550 nm) plotted as a function of areal capacitance (the absolute capacitance for a two-electrode device of equal area is shown on the top axis). The dashed line is a fit to eq 6 and represents bulk-like behavior. Inset: same data plotted as $1-T$ to more clearly show the deviation from bulk-like behavior due to percolation. The solid line is a plot of eq 7 using the constants described in the text and represents percolation. Note that the solid line deviates from the point with lowest C/A due to an approximation in the derivation. (B) Ragone plot comparing the data described in this paper to other transparent supercapacitors described in the literature. The bracket indicates the region of the data dominated by percolation. The arrow indicates the boundary between film with T > 90% and T < 90%.

This concept also allows us to justify our use of eq 5 to describe the capacitance. As the capacitance scales with the surface area of the electrode, we would expect it to be proportional to the fraction of nanotubes connected to the network (*i.e.*, those not isolated like the red rods in Figure 4C). However, percolation theory shows that the probability that a nanotube is connected to the network (*i.e.*, the fraction of nanotubes which are connected) scales as $P \propto (N_A - N_{A,C})^{\beta}$, where β is a scaling exponent.[24] Because we expect $C/A \propto P$, this shows that the capacitance should indeed follow the scaling law described by eq 5.

Electrode Performance. As electrode thicknesses are reduced to increase transmittance, the absolute capacitance falls not only because of percolation but also because the electrode mass scales with thickness. This is important because the energy storage capability of the capacitor is proportional to the capacitance. We explore this trade-off between transmittance and capacitance by plotting the measured transmittance *versus* the areal capacitance in Figure 5A. The absolute capacitance expected for a two-electrode device with

these electrodes is shown on the top axis (taking an electrode area of 2.83 cm^2 and dividing by 2 to correct for 2 electrodes per device). We see that thicker films have high C/A and low T, while thin films display the opposite. For a bulk-like electrode, the areal capacitance is related to the thickness by $C/A = C_{V,B}t$, where $C_{V,B}$ is the bulk-like volumetric capacitance. Combining this with eq 4 to eliminate t gives an equation which relates the transmittance to the areal capacitance for bulk-like electrodes:

$$T = \left[1 + \frac{Z_0\sigma_{Op}}{2C_{V,B}}\frac{C}{A}\right]^{-2} \quad (6)$$

The dashed line in Figure 5A is a fit to this equation. Very good agreement is observed for $Z_0\sigma_{Op}/2C_{V,B}$ = 566 cm^2/F.

We note that the data appear to deviate from the fit line for $C/A < 10^{-4}$ F/cm^2 due to percolation. This can be seen more clearly in the inset which plots $1-T$ *versus* C/A. We can use percolation theory to derive an expression for C/A for films with $t < t_{min,C}$, following the procedure described in ref 29. We can rewrite eq 5, making the approximation $t - t_c \approx t$ and note that, at the percolation to bulk transition, $t = t_{min,C}$ and $C_V = C_{V,B}$, allowing us to write $C_V = C_{V,B}(t/t_{min,C})^{n_C}$, where $C_{V,B}$ is the volumetric capacitance for a bulk-like film. Inserting this expression into $C/A = C_V t$ (true for all thicknesses) gives an equation which can be substituted into eq 4 (eliminating t) to give

$$T = \left[1 + \frac{Z_0\sigma_{Op}t_{min,C}}{2}\left(\frac{C/A}{C_{V,B}t_{min,C}}\right)^{1/(n_C+1)}\right]^{-2} \quad (7)$$

All of the parameters in this expression have been described in this paper, $\sigma_{Op} = 1.7 \times 10^4$ S/m, $t_{min,C} \approx$ 20 nm (Figure 3D), $C_{V,B} \approx 55$ F·cm^{-3} (Figure 4B), and $n_C = 0.83$. Using these known values, we can plot eq 7 on the Figure 5A inset. The result is the solid line and matches the data extremely well. We note that the disagreement between the theoretical line and the data point with smallest C/A is due to the approximation $t - t_c \approx t$.

It is useful to consider what capacitance can be achieved for a film with $T = 90\%$. This can be derived by rearranging eq 7 while setting $T = 90\%$ to give

$$\left(\frac{C}{A}\right)_{T=90\%} = \frac{C_{V,B}}{t_{min,C}^{n_C}}\left(\frac{0.11}{Z_0\sigma_{Op}}\right)^{n_C+1} = C_{V,B}t_{min,C}\left(\frac{0.11}{Z_0\sigma_{Op}t_{min,C}}\right)^{n_C+1} \quad (8)$$

This means that to have high T coupled with high C/A one needs low σ_{Op} and $t_{min,C}$ coupled with high $C_{V,B}$. We note that while σ_{Op} is generally a materials property, both $t_{min,C}$ (ref 29) and $C_{V,B}$ depend on nanotube bundle diameter such that low diameters should give better results. In addition, we note high values of n_C are favorable for high C/A. For electrical percolation, it is known that n_{DC} is controlled by the distribution of junction resistances in the network[38−40] and so scales with network nonuniformity.[31] However, it is not yet clear what parameters control n_C. However, if we assume that n_C also scales with network nonuniformity, the requirement for high n_C would suggest that nonuniform networks are preferred for thin, transparent supercapacitors. However, we note that the sheet resistance (and so the ESR) for percolating networks also scales with n_{DC} (or n_{ESR}).[29,31] This means that networks with high n_C (and so presumably n_{DC}) will have higher C/A but also higher R_{ESR}. This trade-off will need to be considered for particular applications.

The energy density and power density of a symmetric supercapacitor can be calculated using[41]

$$E/M = C_D\Delta V^2/2M \quad (9)$$

and

$$P/M = \Delta V^2/4R_{ESR,D}M \quad (10)$$

where ΔV is the operating voltage (taken as 0.8 V in this case) and M is twice the mass of SWNTs per electrode. We note that the device capacitance, C_D, is half the measured electrode capacitance, while the device ESR, $R_{ESR,D}$, is twice the measured electrode ESR (due to the fact that we work with a three-electrode cell).[15] We have plotted E/M *versus* P/M in Figure 5B. We have also included data reported in the literature for other transparent supercapacitors.[7,10,11] The SCs with bulk-like electrodes prepared here tend to cluster in the top right portion of the graph, while the thinner percolative networks extend down toward the bottom left. We note that all data points to the right of the arrow represent electrodes with $T < 90\%$. It is clear from this graph that our transparent electrodes with thicknesses in the bulk regime behave similarly to transparent electrochemical capacitor electrodes published in the literature. However, importantly, we show that increasing the transparency is accompanied by a rapidly diminishing power and energy densities due to percolative effects.

To maximize power and energy density for high T electrodes, it would be necessary to shift the transition from bulk-like to percolative behavior to lower thickness, that is, $t_{min,ESR}$ and $t_{min,C}$ must be reduced. It is known that $t_{min,DC}$ scales linearly with the diameter of the rods making up the network, in this case the nanotube bundle diameter, and it is reasonable to assume the same for $t_{min,ESR}$ and $t_{min,C}$. Thus, it is possible that percolation effects can be minimized or avoided altogether by using better exfoliated nanotubes. According to Figure 3, $T = 90\%$ can be achieved for $t = 16$ nm. We recently showed that $t_{min,DC} \approx 2.33D$,

where D is the bundle diameter.[29] Thus, the onset of electrical percolation could be suppressed to below $t_{min,DC}$ = 16 nm so long as D < 7 nm.

The data in Figure 5A show that for the tubes used here a transmittance of 90% per electrode (*i.e.*, 81% per capacitor assuming a perfectly transparent electrolyte) limits the attainable areal capacitance to $\sim 10^{-4}$ F/cm^2 per electrode or $\sim 1.5 \times 10^{-4}$ F for a two-electrode device with the area used here. This would be equivalent to a stored energy of $\sim 10^{-4}$ J. We note that due to percolation effects the achievable capacitance/energy is much reduced if T > 90% is required. Without knowing the exact role that transparent capacitors will play, it is difficult to assess whether these energies are large enough for applications. However, we emphasize that much work is currently ongoing into autonomous sensing/communication platforms.[42] These miniature devices will incorporate sensors which can communicate a detection event to the outside world *via* a radio frequency antenna. The communication event is likely to be powered by a supercapacitor which can later be recharged perhaps using photovoltaic technology. Transparency may be an advantage for such integrated devices for reasons of camouflage or to make them unobtrusive for aesthetic reasons. It has been estimated that the energy requirements for communication would be tens of microjoules per event.[43] These power requirements appear to be compatible with the transparent nanostructured supercapacitors described here. It is worth noting that, if more energy is required, the nanotube network could be coated with a pseudocapacitive material such as MnO_x.[44] It has been demonstrated that such Faradaic or hybrid double-layer supercapacitors can yield much higher specific capacitance and energy density than pure electrochemical double-layer capacitors.[45] This will increase the volumetric capacitance, although the percolation effects discussed here will still be present.

CONCLUSIONS

In this work, we have examined the effect of percolation on the properties of supercapacitor electrodes, prepared from thin films of carbon nanotubes. Measurements of the electrode transmittance and sheet resistance as a function of thickness show a distinct transition from percolative to bulk-like behavior as the thickness is increased above 100 nm. Characterization of different thickness nanotube films as supercapacitor electrodes confirmed this behavior. The equivalent series resistance also underwent a percolation to bulk transition at electrode thickness of 100 nm. Interestingly, similar results were observed for the areal capacitance albeit with a lower transition thickness of 20 nm. The DC conductivity, effective ESR conductivity, and volumetric capacitance of thin films were all well described by percolation theory. All data could be described by percolation thresholds of 4.3 nm and critical exponents of n_{DC} = 0.66, n_{ESR} = 0.69, and n_C = 0.83. We found the areal capacitance to be controlled by percolation for electrodes with T > 90%. At T = 90%, the capacitance was 10^{-4} F/cm^2, enough to power burst communication for an integrated sensing device. We found that for bulk-like electrodes the energy and power densities clustered in a well-defined area of the Ragone plot. However, the percolative data formed a long tail toward the bottom left corner of the graph. This work illustrates that, if high transparency is required, a severe cost in both power and energy must be paid. However, that cost can be readily estimated using percolation theory.

METHODS

We prepared dispersions by adding P3 single-walled carbon nanotubes (Carbon Solutions Inc.) to Millipore water such that the nanotube concentration was 1 mg/mL. The dispersion was then subjected to 30 min of high power tip sonication (VibraCell CVX; 750W, 20% 60 kHz) and then left to settle overnight before being centrifuged at 5500 rpm for 90 min. The supernatant was carefully decanted and saved for further use. We measure the concentration after centrifugation by measuring the absorbance spectrum and recording the absorbance per unit cell length, A/l, at 660 nm. The Lambert–Beer law ($A = \alpha Cl$) gives the concentration using the extinction coefficient, α = 3389 mL mg^{-1} m^{-1}.[46]

The resulting dispersions were vacuum-filtered using porous cellulose filter membranes (MF-Millipore membrane, mixed cellulose esters, hydrophilic, 0.025 μm, 47 mm) to give thin films. The thickness of these films was controlled by the volume of dispersion filtered and hence the deposited mass. The deposited films were transferred to polyethylene terephthalate (PET) (or AuPd-coated glass) substrates using heat and pressure as described previously.[3] The cellulose filter membrane was then removed by treatment with acetone vapor and subsequent acetone liquid baths followed by a methanol bath. The final film diameter was 36 mm.

SEM was performed using a Zeiss Ultra plus SEM. Optical transmission spectra were recorded in the visible range (400 to 800 nm) using a Varian Cary 6000i. In all cases, PET was used as the reference. Sheet resistance measurements were made using the four-probe technique with silver electrodes of dimensions and spacings typically of approximately millimeter size and a Keithley 2400 source meter. For electrochemical measurements, all nanotube electrodes had the same shape and lateral dimensions (length and width). This is critical to avoid scatter in the ESR measurements. Electrochemical characterization consisted of cyclic voltammetry and electrochemical impedance spectroscopy using a three-electrode electrochemical cell and Gamry Reference 600 potentiostat. Transparent electrodes were used as the working electrode with a carbon counter electrode and Ag/AgCl (3 M NaCl) reference electrode. The supporting electrolyte used for all characterization was 1.0 M H_2SO_4 (Sigma-Aldrich). We determined the capacitive performance of transparent electrodes by cyclic voltammetry within the potential window 0 to 0.8 V *vs* Ag/AgCl at a scan rate of 50 mV·s^{-1}. We determined the equivalent series resistance of the interface by electrochemical impedance spectroscopy (100 kHz to 100 mHz). An AC perturbation of 10 mV was applied to the interface within the frequency range 0.1 MHz to 10 mHz.

Acknowledgment. We acknowledge the Science Foundation Ireland funded collaboration (SFI grant 03/CE3/M406s1) between Trinity College Dublin and Hewlett-Packard, which has allowed this work to take place. In addition, we recognize the CRANN pathfinder award to develop supercapacitor testing facilities. J.N.C. also acknowledges support from the European Research Council, Grant SEMANTICS and Science Foundation Ireland Grant No. 07/IN.1/I1772. Finally, we acknowledge Dr. Lorraine Byrne of Hewlett-Packard for useful discussions.

REFERENCES AND NOTES

1. Doherty, E.; De, S.; Lyons, P.; Shmeliov, A.; Nirmalraj, P.; Scardaci, V.; Joimel, J.; Blau, W.; Boland, J.; Coleman, J. The Spatial Uniformity and Electromechanical Stability of Transparent, Conductive Films of Single Walled Nanotubes. *Carbon* **2009**, *47*, 2466–2473.
2. Hu, L.; Hecht, D. S.; Gruner, G. Percolation in Transparent and Conducting Carbon Nanotube Networks. *Nano Lett.* **2004**, *4*, 2513–2517.
3. Wu, Z. C.; Chen, Z. H.; Du, X.; Logan, J. M.; Sippel, J.; Nikolou, M.; Kamaras, K.; Reynolds, J. R.; Tanner, D. B.; Hebard, A. F.; *et al.* Transparent, Conductive Carbon Nanotube Films. *Science* **2004**, *305*, 1273–1276.
4. Hecht, D. S.; Hu, L. B.; Irvin, G. Emerging Transparent Electrodes Based on Thin Films of Carbon Nanotubes, Graphene, and Metallic Nanostructures. *Adv. Mater.* **2011**, *23*, 1482–1513.
5. Riedl, T.; Gorrn, P.; Kowalsky, W. Transparent Electronics for See-Through AMOLED Displays. *J. Disp. Technol.* **2009**, *5*, 501–508.
6. Yang, Y.; Jeong, S.; Hu, L. B.; Wu, H.; Lee, S. W.; Cui, Y. Transparent Lithium-Ion Batteries. *Proc. Natl. Acad. Sci. U.S.A.* **2011**, *108*, 13013–13018.
7. Chen, P. C.; Shen, G.; Sukcharoenchoke, S.; Zhou, C. Flexible and Transparent Supercapacitor Based on In_2O_3 Nanowire/Carbon Nanotube Heterogeneous Films. *Appl. Phys. Lett.* **2009**, *94*, 043113.
8. Ge, J.; Cheng, G. H.; Chen, L. W. Transparent and Flexible Electrodes and Supercapacitors Using Polyaniline/Single-Walled Carbon Nanotube Composite Thin Films. *Nanoscale* **2011**, *3*, 3084–3088.
9. Hu, Y.; Zhu, H. W.; Wang, J.; Chen, Z. X. Synthesis of Layered Birnessite-Type Manganese Oxide Thin Films on Plastic Substrates by Chemical Bath Deposition for Flexible Transparent Supercapacitors. *J. Alloys Compd.* **2011**, *509*, 10234–10240.
10. Kaempgen, M.; Chan, C. K.; Ma, J.; Cui, Y.; Gruner, G. Printable Thin Film Supercapacitors Using Single-Walled Carbon Nanotubes. *Nano Lett.* **2009**, *9*, 1872–1876.
11. Yu, A. P.; Roes, I.; Davies, A.; Chen, Z. W. Ultrathin, Transparent, and Flexible Graphene Films for Supercapacitor Application. *Appl. Phys. Lett.* **2010**, *96*, 253105.
12. Chen, P.; Chen, H.; Qiu, J.; Chou, C. Inkjet Printing of Single-Walled Carbon Nanotube/RuO_2 Nanowire Supercapacitors on Cloth Fabrics and Flexible Substrates. *Nano Res.* **2010**, *3*, 594–603.
13. Feng, J.; Sun, X.; Wu, C. Z.; Peng, L. L.; Lin, C. W.; Hu, S. L.; Yang, J. L.; Xie, Y. Metallic Few-Layered VS(2) Ultrathin Nanosheets: High Two-Dimensional Conductivity for In-Plane Supercapacitors. *J. Am. Chem. Soc.* **2011**, *133*, 17832–17838.
14. Yoo, J. J.; Balakrishnan, K.; Huang, J. S.; Meunier, V.; Sumpter, B. G.; Srivastava, A.; Conway, M.; Reddy, A. L. M.; Yu, J.; Vajtai, R.; *et al.* Ultrathin Planar Graphene Supercapacitors. *Nano Lett.* **2011**, *11*, 1423–1427.
15. Zhang, L. L.; Zhao, X. S. Carbon-Based Materials as Supercapacitor Electrodes. *Chem. Soc. Rev.* **2009**, *38*, 2520–2531.
16. Frackowiak, E. Carbon Materials for Supercapacitor Application. *Phys. Chem. Chem. Phys.* **2007**, *9*, 1774–1785.
17. Niu, C. M.; Sichel, E. K.; Hoch, R.; Moy, D.; Tennent, H. High Power Electrochemical Capacitors Based on Carbon Nanotube Electrodes. *Appl. Phys. Lett.* **1997**, *70*, 1480–1482.
18. Simon, P.; Gogotsi, Y. Materials for Electrochemical Capacitors. *Nat. Mater.* **2008**, *7*, 845–854.
19. Stoller, M. D.; Park, S. J.; Zhu, Y. W.; An, J. H.; Ruoff, R. S. Graphene-Based Ultracapacitors. *Nano Lett.* **2008**, *8*, 3498–3502.
20. Futaba, D. N.; Hata, K.; Yamada, T.; Hiraoka, T.; Hayamizu, Y.; Kakudate, Y.; Tanaike, O.; Hatori, H.; Yumura, M.; Iijima, S. Shape-Engineerable and Highly Densely Packed Single-Walled Carbon Nanotubes and Their Application as Super-Capacitor Electrodes. *Nat. Mater.* **2006**, *5*, 987–994.
21. Izadi-Najafabadi, A.; Yasuda, S.; Kobashi, K.; Yamada, T.; Futaba, D. N.; Hatori, H.; Yumura, M.; Iijima, S.; Hata, K. Extracting the Full Potential of Single-Walled Carbon Nanotubes as Durable Supercapacitor Electrodes Operable at 4 V with High Power and Energy Density. *Adv. Mater.* **2010**, *22*, E235–E241.
22. Stoller, M. D.; Ruoff, R. S. Best Practice Methods for Determining an Electrode Material's Performance for Ultracapacitors. *Energy Environ. Sci.* **2010**, *3*, 1294–1301.
23. Kaempgen, M.; Chan, C. K.; Ma, J.; Cui, Y.; Gruner, G. Printable Thin Film Supercapacitors Using Single-Walled Carbon Nanotubes. *Nano Lett.* **2009**, *9*, 1872–1876.
24. Stauffer, D.; Aharony, A. *Introduction to Percolation Theory*, 2nd ed.; Taylor & Francis: London, 1985.
25. Scardaci, V.; Coull, R.; Coleman, J. N. Very Thin Transparent, Conductive Carbon Nanotube Films on Flexible Substrates. *Appl. Phys. Lett.* **2010**, *97*, 023114.
26. De, S.; Coleman, J. N. The Effects of Percolation in Nanostructured Transparent Conductors. *MRS Bull.* **2011**, *36*, 774–780.
27. De, S.; Higgins, T. M.; Lyons, P. E.; Doherty, E. M.; Nirmalraj, P. N.; Blau, W. J.; Boland, J. J.; Coleman, J. N. Silver Nanowire Networks as Flexible, Transparent, Conducting Films: Extremely High DC to Optical Conductivity Ratios. *ACS Nano* **2009**, *3*, 1767–1774.
28. De, S.; King, P. J.; Lotya, M.; O'Neill, A.; Doherty, E. M.; Hernandez, Y.; Duesberg, G. S.; Coleman, J. N. Flexible, Transparent, Conducting Films of Randomly Stacked Graphene from Surfactant-Stabilized, Oxide-Free Graphene Dispersions. *Small* **2010**, *6*, 458–464.
29. De, S.; King, P. J.; Lyons, P. E.; Khan, U.; Coleman, J. N. Size Effects and the Problem with Percolation in Nanostructured Transparent Conductors. *ACS Nano* **2010**, *4*, 7064–7072.
30. Unalan, H. E.; Fanchini, G.; Kanwal, A.; Du Pasquier, A.; Chhowalla, M. Design Criteria for Transparent Single-Wall Carbon Nanotube Thin-Film Transistors. *Nano Lett.* **2006**, *6*, 677–682.
31. Scardaci, V.; Coull, R.; Lyons, P. E.; Rickard, D.; Coleman, J. N. Spray Deposition of Highly Transparent, Low-Resistance Networks of Silver Nanowires over Large Areas. *Small* **2011**, *7*, 2621–2628.
32. Dressel, M.; Gruner, G. *Electrodynamics of Solids*; Cambridge Press: Cambridge, UK, 2002.
33. Geng, H. Z.; Lee, D. S.; Kim, K. K.; Han, G. H.; Park, H. K.; Lee, Y. H. Absorption Spectroscopy of Surfactant-Dispersed Carbon Nanotube Film: Modulation of Electronic Structures. *Chem. Phys. Lett.* **2008**, *455*, 275–278.
34. Ruzicka, B.; Degiorgi, L.; Gaal, R.; Thien-Nga, L.; Bacsa, R.; Salvetat, J. P.; Forro, L. Optical and DC Conductivity Study of Potassium-Doped Single-Walled Carbon Nanotube Films. *Phys. Rev. B* **2000**, *61*, R2468–R2471.
35. Ugawa, A.; Hwang, J.; Gommans, H. H.; Tashiro, H.; Rinzler, A. G.; Tanner, D. B. Far-Infrared to Visible Optical Conductivity of Single-Wall Carbon Nanotubes. *Curr. Appl. Phys.* **2001**, *1*, 45–49.
36. Luo, H.; Shi, Z.; Li, N.; Gu, Z.; Zhuang, Q. Investigation of the Electrochemical and Electrocatalytic Behavior of Single-Wall Carbon Nanotube Film on a Glassy Carbon Electrode. *Anal. Chem.* **2001**, *73*, 915–920.
37. Geng, H. Z.; Kim, K. K.; So, K. P.; Lee, Y. S.; Chang, Y.; Lee, Y. H. Effect of Acid Treatment on Carbon Nanotube-Based Flexible Transparent Conducting Films. *J. Am. Chem. Soc.* **2007**, *129*, 7758–7759.
38. Balberg, I. Tunnelling and Nonuniversal Conductivity in Composite-Materials. *Phys. Rev. Lett.* **1987**, *59*, 1305–1308.

39. Grimaldi, C.; Balberg, I. Tunneling and Nonuniversality in Continuum Percolation Systems. *Phys. Rev. Lett.* **2006**, *96*, 066602.
40. Johner, N.; Grimaldi, C.; Balberg, I.; Ryser, P. Transport Exponent in a Three-Dimensional Continuum Tunneling-Percolation Model. *Phys. Rev. B* **2008**, *77*, 174204.
41. Zhang, L. L.; Zhao, X. S. Carbon-Based Materials as Supercapacitor Electrodes. *Chem. Soc. Rev.* **2009**, *38*, 2520–2531.
42. Sample, A. P.; Yeager, D. J.; Powledge, P. S.; Mamishev, A. V.; Smith, J. R. Design of an RFID-Based Battery-Free Programmable Sensing Platform. *IEEE Trans. Instrum. Meas.* **2008**, *57*, 2608–2615.
43. Roy, S.; Jandhyala, V.; Smith, J. R.; W etherall, D. J.; Otis, B. P.; Chakraborty, R.; Buettner, M.; Yeager, D. J.; Ko, Y.-C.; Sample, A. P. RFID: From Supply Chains to Sensor Nets. *Proc. IEEE* **2010**, *98*, 1583–1592.
44. Kim, J. H.; Lee, K. H.; Overzet, L. J.; Lee, G. S. Synthesis and Electrochemical Properties of Spin-Capable Carbon Nanotube Sheet/MnO(x) Composites for High-Performance Energy Storage Devices. *Nano Lett.* **2011**, *11*, 2611–2617.
45. Conway, B. E. *Electrochemical Supercapacitors: Scientific Fundamentals and Technological Applications*; Springer: Berlin, 1997; p 736.
46. Bergin, S. D.; Nicolosi, V.; Cathcart, H.; Lotya, M.; Rickard, D.; Sun, Z.; Blau, W. J.; Coleman, J. N. Large Populations of Individual Nanotubes in Surfactant-Based Dispersions without the Need for Ultracentrifugation. *J. Phys. Chem. C* **2008**, *112*, 972–977.